Available online at www.sciencedirect.com
ScienceDirect
Tectonophysics 445 (2007) 210–226
TECTONOPHYSICS
www.elsevier.com/locate/tecto

Seismic properties of the upper crust in the central Friuli area (northeastern Italy) based on petrophysical data

M. Faccenda [a,*], G. Bressan [b], L. Burlini [c]

[a] Institute of Geophysics, HPP L 12, ETH Hönggerberg, 8093 Zürich, Switzerland
[b] Dip. Centro Ricerche Sismologiche - Istituto Nazionale di Oceanografia e Geofisica Sperimentale, Udine, Via Treviso 55, Cussignacco, 33100 Udine, Italy
[c] Geological Institute, LEB D 4, Leonhardstrasse 19, ETH Zentrum, 8092 Zürich, Switzerland

Received 22 March 2007; received in revised form 20 July 2007; accepted 6 August 2007
Available online 10 August 2007

Abstract

The compressional and shear wave velocities have been measured at room temperature and pressure up to 450 MPa on 5 sedimentary rock samples, representative of the most common lithologies of the upper crust in the central Friuli area (northeastern Italy). At 400 MPa confining pressure the Triassic dolomitic rock shows the highest velocities (Vp ~7 km/s, Vs ~3.6 km/s), the Jurassic and Triassic limestones samples intermediate velocities (Vp ~6.3 /s, Vs ~3.5 km/s) and the Cenozoic and Paleozoic sandstones the lowest velocities (Vp ~6.15 km/s, Vs ~3.35 km/s). The Paleozoic sandstone sample is characterized by the strongest anisotropy (10%) and significant birefringence (0.2 km/s) is found only on the Cenozoic sandstone sample. We elaborated the synthetic profiles of seismic velocities, density, elastic parameters and reflection coefficient, related to 4 one-dimensional geological models extended up to 22 km depth. The synthetic profiles evidence high rheological contrasts between Triassic dolomitic rocks and the soft sandstones and the Jurassic limestones. The Vp profiles obtained from laboratory measurements match very well the in-situ Vp profile measured by sonic log for the limestones and dolomitic rocks, supporting our one-dimensional modelling of the calcareous-carbonatic stratigraphic series. The Vp and Vs values of the synthetic profiles are compared with the corresponding ones obtained from the 3-D tomographic inversion of local earthquakes. The laboratory Vp are generally higher than the tomographic ones with major discrepancies for the dolomitic lithology. The comparison with the depth location of seismicity reveals that the seismic energy is mainly released in correspondence of high-contrast rheological boundaries.

Keywords: Petrophysics; Laboratory measurements; Vp; Vs; Seismic properties; Seismicity; Sonic log

1. Introduction

The interpretation of geophysical results in terms of nature and structure of the lithosphere mainly relies on the physical properties of rocks measured on samples from exposed crustal sections (e.g. Fountain, 1976), boreholes (e.g. Siegesmund, 1996) or xenoliths (e.g. Kern et al., 1996). No direct correlation has been made between lithology, structure and, for instance, seismic velocity. Therefore the interpretation of seismic structures is not unique (Rudnick and Fountain, 1995). We know from laboratory experiments that several parameters affect the physical properties of rocks: some are intrinsic (e.g. rock

* Corresponding author. Tel.: +41 44 63 37653; fax: +41 44 63 31065.
E-mail addresses: faccenda@erdw.ethz.ch (M. Faccenda), gbressan@inogs.it (G. Bressan), luigi.burlini@erdw.ethz.ch (L. Burlini).

0040-1951/$ - see front matter © 2007 Elsevier B.V. All rights reserved.
doi:10.1016/j.tecto.2007.08.004

fabric, mineralogy, microfracturing) and some are extrinsic (pressure, temperature and pore fluid pressure). In practice, a specific velocity of propagation of compressional wave can be obtained on different lithologies by applying different P, T or P_{fluid} conditions, or varying the intrinsic rock properties. Therefore a better definition of the effects that confining pressure, temperature and pore fluid pressure have on the physical properties of rocks is required for a better geophysical interpretation of crustal and lithospheric structures.

Recently, the upper crustal structure of the Friuli area was investigated by Gentile et al. (2000) using the tomographic joint inversion for hypocenters and 3-D velocity structure from local earthquakes and the modelling of gravity anomalies. This study related the 3-D Vp and Vp/Vs images to the main lithological units, the tectonic pattern and the seismicity. However, also in this case the geological interpretation is not unique since many rock types are characterized by similar velocities and the 3-D tomographic images are not well resolved everywhere. Furthermore, the seismic intrinsic properties of the rock units that compose the upper crust of the Friuli area involved with the seismicity are still unknown.

In the present paper we investigate the seismic properties of the most representative lithologies of the Friuli upper crust starting by the laboratory measurements of the compressional and shear wave velocities up to high confining pressure. The high pressures in laboratory measurements are necessary because they allow the separation between the crack-induced seismic properties from the matrix properties (e.g. Rasolofosaon et al., 2000). The seismic intrinsic properties are used to construct the synthetic profiles of seismic velocities, density, elastic parameters and reflection coefficients of 4 one-dimensional geological models, extended up to 22 km depth. It is often argued that the small samples used for the experiments might not be sufficient to represent the large scale properties. Therefore we compared the results with the sonic log data from a borehole in the area, in the same was as Dey-Barsukov et al. (2000) or Rasolofosaon et al. (2000), as well as from the tomography (Gentile et al., 2000). In the end, the synthetic profiles are compared with the depth profiles of the released seismic energy to explore the relation between the occurrence of seismicity and the crustal seismic properties.

2. Geological framework

2.1. Tectonic structure

The Friuli area is characterized by a complex tectonic pattern, resulting from the superposition of several Cenozoic-age tectonic phases (Fig. 1a). The structural framework is mainly characterized by two indented tectonic wedges, in which the outer surrounds the inner wedge (Fig. 1b); these wedges are outlined by NE–SW and NW–SE orientated paleo-fault systems (Venturini, 1991). They were formed from Paleozoic to the middle Eocene times by syn-sedimentary tectonic movements and they were re-activated during the compressional Cenozoic tectonic phases. The Mesoalpine (Dinaric) NE–SW compression was the earliest tectonic phase and generated NW–SE-orientated thrusts during the Middle–late Eocene, mainly in Slovenia and in the southeastern part of the Friuli area. During the middle to the earliest Pliocene, the north–south-trending Alpine compression caused severe shortening of the upper crust (Castellarin, 1979) and formed south-verging thrusts and backthrusts, orientated almost E–W, recognizable in the central part of the area. The last tectonic phase was a NW–SE-orientated compression during the Pliocene times. It generated NE–SW-trending thrusts and folds, mainly recognizable in the northwestern part of the area. Each tectonic phase inherited the deformations of the previous phase and fragmented the crust into different tectonic domains; this complexity is revealed by the strong lateral heterogeneities of Vp and Vp/Vs tomographic images of Gentile et al. (2000).

2.2. Geological setting

The geological setting of the Friuli area (Slejko et al., 1989) is characterized by sedimentary rocks ranging from Paleozoic to Quaternary age (Fig. 1a). The Paleozoic rocks, that outcrop in the northern part of the area, are mainly composed by terrigenous and volcanic deposits and minor limestones. The geologic units of the central part of the area are mainly made up of limestones and carbonatic rocks (Triassic–Cretaceous age), belonging to the thick shelf complex of the Friuli Platform (Bosellini, 2004). Flysch and molasse compose the Cenozoic and Quaternary deposits.

The central part of the Friuli area, where the synthetic profiles of seismic velocities and elastic moduli were elaborated, is mainly characterized by the Mesozoic limestones and carbonatic rocks. The Mesozoic cover is detached from the Paleozoic geologic units as consequence of the severe shortening caused by the north–south-trending Alpine compression. The dominant tectonic pattern is a south-verging embricated structure of folds and thrusts dipping 40° to 60° with some associated backthrusts (Fig. 1a). The thrusting caused alternations and repetitions of the Triassic dolomitic rocks and Jurassic limestones (Carulli and Ponton, 1992).

For our purpose, we elaborated 4 schematic one-dimensional geological models (Fig. 4, located in S1 to S4 in Fig. 1a) which are representative of the central Friuli area. These geological models were elaborated according to Vai et al. (2002) for the lithostratigraphic sequence and according to the geological cross-sections of Carulli and Ponton (1992), Merlini et al. (2002) and Poli et al. (2002) for the geometry and the thickness of

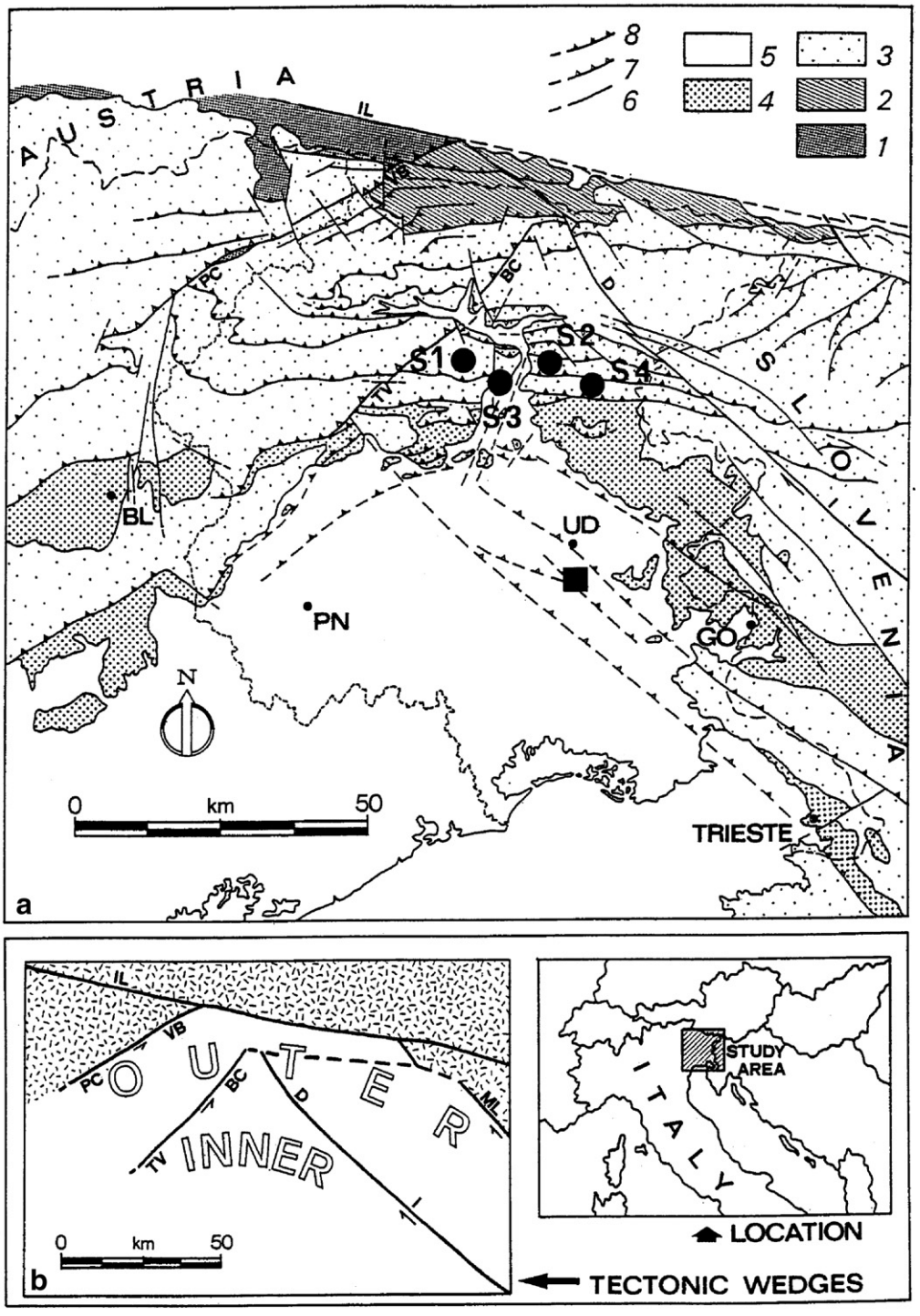

the sedimentary units. In detail, the weakly metamorphosed sandstones of the Hockwipfel Formation (Fm.) were considered the most representative and predominant lithologies of the Paleozoic units (Martinis, 1993).

As emphasized above, the severe shortening of the overlying Mesozoic cover, caused by thrusting, produced frequent repetitions and thickening of the sedimentary units, evidenced by the geological cross-sections here considered. The lower–middle Triassic age units are mainly composed of limestones that we represent with the limestone of the Werfen Fm. The thickness of these limestones varies from 1 to about 3 km. The whole Mesozoic sequence is mainly made up of the middle–upper Triassic dolomitic rock of the Dolomia Principale Fm., which is also the most frequent repeated unit. In some geological sections the layers of the Dolomia Principale Fm. are about 3 km thickened. The thickness of the Jurassic limestones varies from 1 to about 2 km while the Cretaceous limestones are less diffuse with maximum thickness about 1 km. The Jurassic–Cretaceous limestones are here represented by the Calcari Grigi Fm. The Tertiary deposits, recognizable only in the S4 profile, has maximum thickness 1 km and are represented by the sandstones of the Alpine Flysch.

The rock types selected as representative of the sedimentary cover of the central Friuli area represent roughly 90% of the total volume of rocks. The other rock types of the stratigraphic sequence, not considered in our geological models, are clastic deposits and evaporites of Permian–lower Triassic age, with variable thickness (about one hundred meters) and minor calcareous Formations of the Jurassic period.

We consider also for our one-dimensional modelling the stratigraphic sequence (Venturini, 2002), outlined by the well Cargnacco 1 (Fig. 1). It represents, as discussed in Section 6.1, an important test for the validity of our schematic modelling of the upper Triassic–Cretaceous limestones.

The crystalline basement (Cati et al., 1987) underlying the Paleozoic deposits is modelled with granodioritic orthogneiss (Mazzoli et al., 2002). The depth boundary between the Paleozoic rocks and the crystalline basement occurs at about 15 km and it is marked by an increase of crustal Vp velocities from about 6.0 km/s to 6.4 km/s, according to Scarascia and Cassinis (1997).

2.3. Sample description

The main petrographic features of the analyzed samples (Fig. 2) are briefly reported below:

Sample 1 (from the Hockwipfel formation) is a weakly metamorphosed sandstone belonging to the Paleozoic basement *s.l.* (Fig. 2a). The mineral assemblage is quartz, Na-plagioclase, muscovite and chlorite. Macroscopically it exhibits a well developed foliation defined by the preferred orientation of the mica flakes and a lineation defined by the elongation of quartz grains. The grainsize is not uniform ranging from 10 to 400 μm. Several dissolution planes are outlined by alignment of opaque minerals and by the strain grain boundaries of many quartz grains, suggesting that the main deformation mechanism was dissolution and precipitation creep.

Sample 2 (from the Werfen formation) is a limestone with flattened calcite grains defining the foliation (Fig. 2b). Quartz crystals are rarely present. The grainsize is not uniform, with porphyroclasts of calcite surrounded by smaller calcite grains (core and mantle structure). The calcite porphyroclasts are heavily twinned, with thin parallel sided twins, suggesting a temperature below 200 °C during the deformation (Ferrill et al., 2004). These grains also present undulose extinction, suggesting that the main deformation mechanism responsible of the strong fabric was dislocation creep associated to the twinning. The newly formed small grains at the rim of the porphyroclasts are equidimensional and without undulose extinction. These features suggest incipient dynamic recrystallization during the deformation.

Sample C2 (from the Dolomia Principale formation) is a fine-grained dolomitic rock with some calcitic veins (Fig. 2c). It exhibits a very weak foliation. The dolomite grains are fine grained and sometime contain larger calcitic grains (probably the filling of fossils). Some calcite veins demonstrate a brittle deformation phase with millimetric scale dislocation patterns. The calcite grains filling the veins (Fig. 2c) are equidimensional and

Fig. 1. a — Schematic geology of the eastern Southern Alps (from Bressan et al., 2003). 1) Hercynian very-low metamorphic basement (Ordovician–Carboniferous). 2) Paleocarnic Chain, non-and anchimetamorphic succession (Upper Ordovician–Carboniferous). 3) Upper Carboniferous and Permo–Mesozoic carbonate successions. 4) Flysch (Upper Maastrichtian–Middle Eocene) and molassic sequence (Miocene). 5) Quaternary covers. 6) Subvertical fault. 7) Reverse fault, sometimes ancient syn-sedimentary fault reactivated as compressional fault. 8) Thrust. PC–VB: Pieve di Cadore and Val Bordaglia lines; TV–BC: Tramonti–Verzegnis and But–Chiarsò lines; D–I: Dogna and Idria lines; IL: eastern Insubric lineament (Gailtal line); ML: Mojstrana and Ljubljana lines. BL: Belluno; PN: Pordenone; UD: Udine; GO: Gorizia. b — The inset shows the two indented tectonic wedges as depicted by the faults described above, enhanced by capital letters. The strike slip was active during the Neoalpine N–S-trending compression. S1, S2, S3 and S4 are the location of the stratigraphic synthetic profiles. The square shows the location of the well Cargnacco 1 of the ENI-AGIP Company.

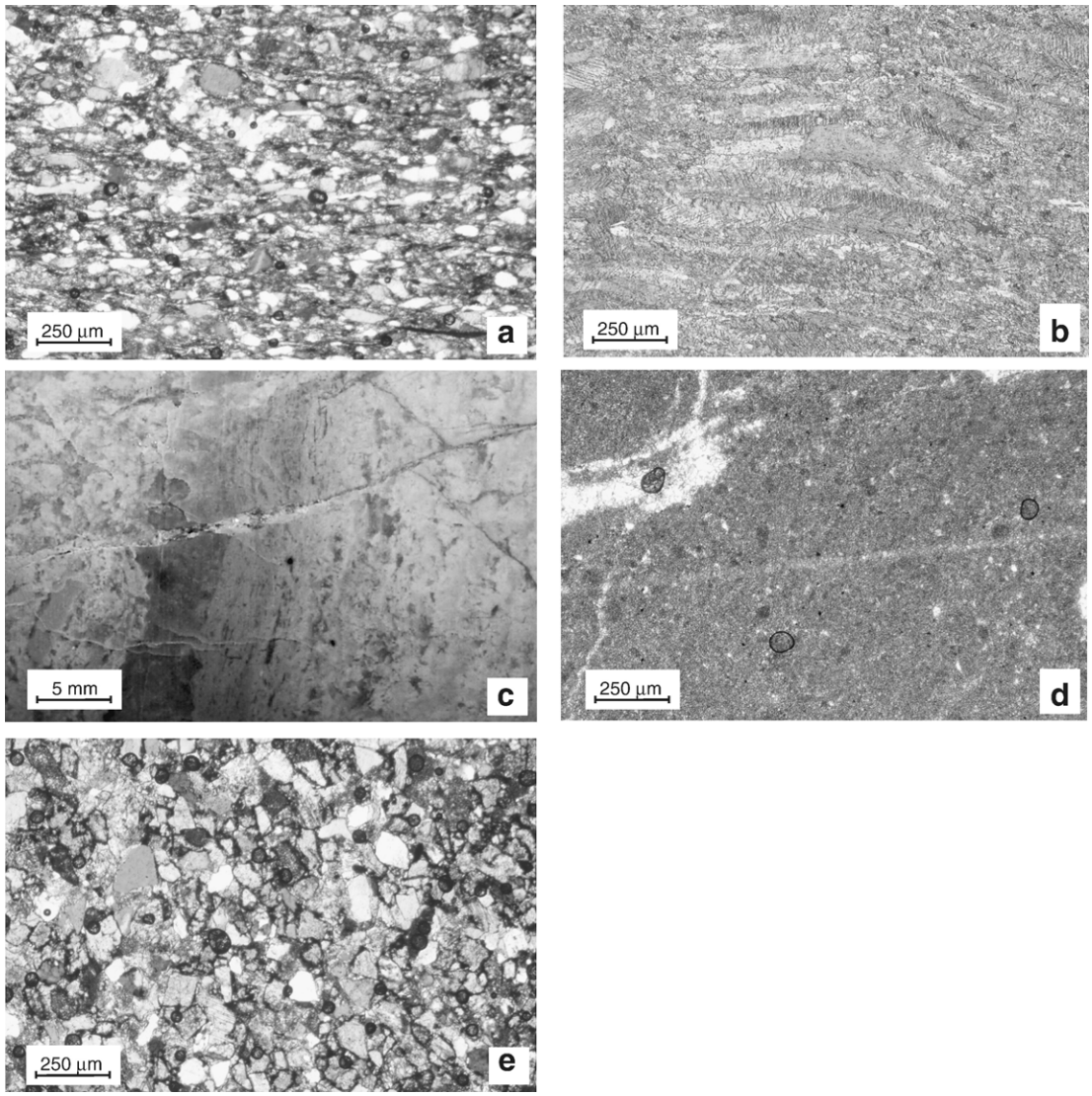

Fig. 2. a, b, d, e: — Cross-polarized microphotographs (X–Z plane) of: a) sample 1: Paleozoic sandstone (Fm. Hockwipfel); b) sample 2: Triassic limestone (Fm. Werfen); d) sample C1: Jurassic–Cretaceous limestone (Fm. Calcari Grigi); e) sample 4: Cenozoic sandstone (Alpine Flysch). c) photograph of the bulk core of the sample C2: Triassic dolomite Fm. Dolomia Principale); the long edge is the Z direction (core axis).

of large grainsize. They rarely exhibit twinning, suggesting that the vein filling was not followed by any further deformation. The sample seems therefore isotropic from the small scale fabric, even if a lamination can be observed on the hand specimen.

Sample C1 (from the Calcari Grigi formation) is a fine-grained limestone with some calcitic veins (Fig. 2d) composed mainly by calcite with minor opaques; it shows a weak foliation which is outlined by the flattening of some calcite grains and a vague lineation. The matrix is very fine grained with grainsize ranging from 5 to 20 µm. The opaque minerals are aequant and homogeneously dispersed in the matrix. Different generation of calcite veins can be recognized, some of which strongly deformed. The largest (and latest) veins contain large (millimetric) calcite grains, some of which are twinned, suggesting that even the last veining filling was affected by deformation.

Sample 4 (from the Cenozoic Flysch) is a calcarenite composed of calcite, dolomite, quartz and rarely Na-plagioclase (Fig. 2e). Macroscopically it shows a very weak foliation. The foliation can be only attributed to the preferred alignment of some quartz and mica grains, but microscopically the rock is almost isotropic. The

Table 1
Mineralogical composition of the selected samples with the corresponding uncertainties of the XRD method (σ)

Rock type	Minerals															
	Albite	σ	Ankerite	σ	Calcite	σ	Chlorite	σ	Dolomite	σ	Muscovite	σ	Quartz	σ	Talc	σ
Cenozoic sandstone (4)	2.02	0.32	12.52	0.35	36.79	0.26	–		26.01	0.35	–		22.66	0.24	–	
Calcari Grigi (C1)	–		–		100		–		–		–		–		–	
Dolomia Principale (C2)	0.22	0.09	–		–		–		98.94	0.005	–		–		0.84	0.11
Werfen (2)	–		–		90.04	0.07	–		–		–		9.96	0.23	–	
Hochwipfel (1)	22.69	0.6	–		–		13.97	0.59	–		28.31	1.03	22.66	0.24	–	

grainsize is uniform ranging from 100 to 400 μm. The cement is made of fine grained calcite. Very few calcite grains display deformation twins, indicating that the rock is almost undeformed.

The mineralogical composition of the studied samples has also been determined from XRD (X-Ray Powder Diffraction) quantitative analyses. The results are summarized in Table 1. Diffraction profiles were collected with a Bruker AXS D8 Advance diffractometer and analysed using the Rietveld (whole-profile) method. For this purpose, the GSAS software package (Larson and Von Dreele, 2004) together with EXPGUI interface (Toby, 2001) were used.

3. Experimental techniques

Seismic velocities were measured at room temperature and pressure up to 450 MPa in a *Paterson* gas apparatus at the laboratory of experimental rock deformation at ETH, Zurich, using the pulse transmission technique (Birch, 1960). Cores (25mm in diameter, 20 to 45 mm in length) were drilled along the macroscopic structural directions, i.e. parallel and perpendicular to the lineation (*X* and *Y*, respectively), and normal to the foliation (Z). Both P- and S-wave were measured. Shear waves were measured with the polarization both parallel and perpendicular to foliation or to lineation.

Each side of the cores was prepared smooth and parallel; specimens were oven dried at temperature of 80 °C for at least one day. Bulk densities were measured using dimensions (±0.01 μm) and weights (±0.1 mg), whilst grain densities were determined with a helium-gas pycnometer before (Table 2) and after the seismic wave velocities measurements. As the difference between the two measured effective densities is negligible, no substantial pore collapse was caused by the high pressure experiments.

The ultrasonic compressional and shear waves were generated with lead zirconate titanate piezoelectric transducers of 1MHz resonant frequency. The whole column was jacketed with a copper tube to ensure isolation from the argon gas used as confining medium.

Pressure values over 350 MPa have ±1 MPa of uncertainty; travel times were measured with an oscilloscope with less than 1% of error. Arrival times were obtained with

Table 2
Measured weight, bulk volume, bulk density, effective volume, effective density and porosity at room pressure e temperature; standard deviations account for error propagation formulas

Rock samples	Cores	Weight	Bulk Volume	S.D.	Bulk density	S.D.	Eff. Volume	S.D.	Eff. Density	S.D.	Porosity (%)	S.D.
		g	cm^3		$\rho = P/V_{tot}$ (g/cm^3)		cm^3		$\rho = P/V_{eff}$ (g/cm^3)		$n = [(V_{tot} - V_{eff})/V_{tot}]$	
Cenozoic	4X	51.5293	19.4824	0.8266	2.64	0.11	18.857	0.05	2.73	0.01	3.2	0.0
Sandstone (4)	4Z	53.0508	19.4524	0.2751	2.73	0.04	19.2723	0.05	2.75	0.01	0.9	0.0
Calcari Grigi	C1X	49.691	18.87	1.6012	2.63	0.22	18.6	0.05	2.67	0.01	1.4	0.1
(C1)	C1Y	52.6904	19.837	1.1224	2.66	0.15	19.7522	0.05	2.67	0.01	0.4	0.1
	C1Z	43.6456	16.3867	0.4636	2.66	0.08	16.3768	0.01	2.67	0.00	0.1	0.0
Dolomia Principale (C2)	C2Z	54.902	19.4	0.5488	2.83	0.08	18.411	0.02	2.86	0.00	5.1	0.0
Werfen (2)	2X	53.152	19.7196	0.2789	2.70	0.04	19.5777	0.02	2.71	0.00	0.7	0.0
	2Z	46.8503	17.4755	0.0000	2.68	0.00	17.2763	0.03	2.71	0.00	1.1	0.0
Hochwipfel (1)	1X	30.6462	11.5837	1.9658	2.65	0.45	11.4826	0.01	2.67	0.00	0.9	0.2
	1Z	51.0265	19.0731	0.2699	2.68	0.04	18.8666	0.01	2.70	0.00	1.1	0.0

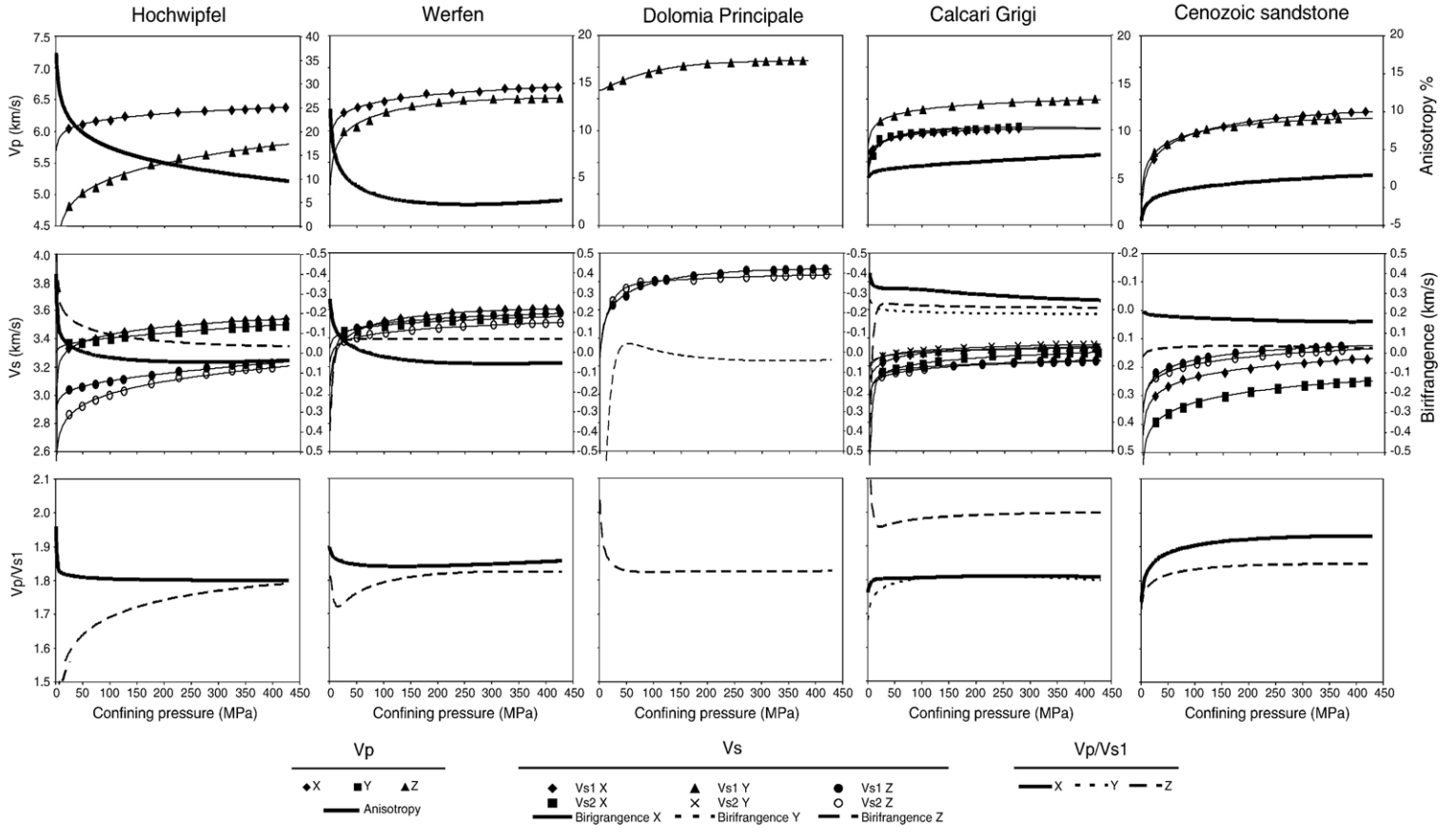

Fig. 3. From left to right, confining pressure vs. Vp, Vs and Vp/Vs ratio of the Hochwipfel, Werfen, Dolomia Principale, Calcari Grigi and Cenozoic sandstone samples, respectively. Full symbols represent measurements during depressurization and are interpolated with lines calculated from Wepfer and Christensen (1991). The thick solid lines are anisotropy and birifrangence, and refer to the vertical axes on the right.

Table 3a
Mean compressional and shear velocities of the selected samples at different confining pressures

Confining pressure (Mpa)									
Rock samples	50	100	150	200	250	300	350	400	450
Compressional wave velocities									
Cenozoic sandstone (4)	5.79	5.96	6.06	6.12	6.16	6.20	6.22	6.24	6.25
Calcari Grigi (C1)	6.00	6.08	6.12	6.14	6.16	6.17	6.17	6.18	6.18
Dolomia Principale (C2)	6.79	6.91	6.98	7.03	7.06	7.08	7.09	7.09	7.10
Werfen (2)	6.24	6.37	6.45	6.50	6.53	6.56	6.58	6.60	6.61
Hochwipfel (1)	5.56	5.72	5.81	5.88	5.94	5.99	6.03	6.07	6.10
Shear wave velocities									
Cenozoic sandstone (4)	3.13	3.19	3.23	3.25	3.27	3.28	3.29	3.30	3.31
Calcari Grigi (C1)	3.24	3.26	3.28	3.29	3.29	3.30	3.30	3.31	3.31
Dolomia Principale (C2)	3.71	3.79	3.83	3.85	3.87	3.88	3.88	3.89	3.89
Werfen (2)	3.46	3.51	3.53	3.55	3.57	3.57	3.58	3.59	3.59
Hochwipfel (1)	3.22	3.27	3.30	3.32	3.34	3.35	3.37	3.38	3.40

a manual picking operation. Calibration were performed using a single sapphire crystal cut parallel to the *c* axis or using a set of brass cylinders of different length. The calibration using the sapphire crystal gave the best results.

4. Results

According to Burke (1987), only measurements taken during depressurisation are reproducible within error limits. Because during preparation there may be induced some minor cracking and, furthermore, some of the cracks and pore spaces do not immediately reopen during depressurisation, the most reliable experimental data are those obtained during depressurisation (Burlini and Kunze, 2000). For this reason, only measurements during depressurization were used for the final processing.

Measurements were taken at 25 and 50 MPa pressure decrements and fitted with the equation reported in Wepfer and Christensen (1991). The velocity increase with increasing pressure (Fig. 3 and Table 3a) in the low pressure range is generally interpreted as due to crack and pore closure (Birch, 1961), whilst the linear part (confining pressure >150–200 MPa) reflects the intrinsic properties of the rocks, and was used to calculate the pressure derivatives.

The seismic velocities of each sample depend primarily on the mineralogical composition and porosity, and only secondarily to grain size. We observed that rocks of the same lithology (i.e., calcite rich samples 2 and C1 or sandstones 1 and 4, see Fig. 2) and with large grains (2 and 4) have higher velocities than those with small grain size (C1 and 1), probably because of less boundary discontinuities along the wave path, thought other mechanisms, like a different rock fabric reflected by the different anisotropic pattern and a different mineralogical composition, could explain such a behavior. The dolomitic rock C2 shows the highest velocities (Vp ~7 km/s, Vs ~3.6 km/s, at 400 MPa), limestones samples 2 and C1 intermediate velocities (Vp ~6.3 km/s, Vs ~3.5 km/s, 400 MPa) and the sandstones 1 and 4 the lowest velocities (Vp ~6.15 km/s, Vs ~3.35 km/s, 400 MPa). The Vp/Vs and Poisson's ratios are consistent with data reported in the literature (Pickett, 1963; Tatham and McCormack, 1991), and depend on the lithology and on the age of the formation, that we interpret as reflecting the degree of cementation (Sheriff and Geldart, 1995); the Paleozoic sandstone shows in fact the lowest value (1.79, Table 3b). It is noteworthy that the composition of the cement, here not analyzed, can affect both the seismic velocities and their ratio; on the other hand, the effect of porosity and pore geometry should be negligible or null at pressures well above the corresponding pore and microfractures closing depth (150–200 MPa), as those of the reported values (400 MPa) (Mavko et al., 1998).

Confining pressures at which the closure of microfractures and pores occur varies between 150 to 200 MPa; at higher confining pressures, the pressure derivatives were higher for the sandstones then the carbonatic samples.

The bulk compressibility, shear modulus and Poisson's ratio were calculated from the measured velocities and densities. The highest values of compressibility and shear modulus were observed for the dolomite (Table 4).

In order to constrain the measured seismic velocities and densities, seismic properties were also calculated using the single crystal elastic constants and the densities reported in Bass (1995), and the volume fractions using the Voigt, Reuss, Hill and Hashin–

Table 3b
Measured effective densities, velocities, anisotropy, birifrangence, Vp vs. Vs1 ratio and pressure and temperature derivatives of velocities at 400 MPa

Rock type	Density (g cm−3)	Vp (x)	Vp (y)	Vp (z)	Vp (xyz)	Anis. (%)	Vs1 (x)	Vs1 (y)	Vs1 (z)	Vs1 (xyz)	Birifrangence (km/s) x	y	z	Vp (xyz)/ Vs1 (xyz)	dVp (xyz)/ dP (10^{-4} km s^{-1} Mpa^{-1})	dVs1 (xyz)/ dP (10^{-4} km s^{-1} Mpa^{-1})	dVp(xyz)/ dT (10^{-4} km s^{-1} K^{-1})	dVs1(xyz)/dT (10^{-4} km s^{-1} K^{-1})
Cenozoic sandstone (4)	2.74	6.29	–	6.19	6.24	1.56	3.26	–	3.35	3.3	0.2	–	0	1.89	5.44	2.41	-1.1×10^{-4}	-5.7×10^{-4}
Calcari Grigi (C1)	2.67	6.02	6.03	6.47	6.18	7.27	3.33	3.35	3.24	3.31	0	0	0	1.87	1.45	0.95	-3.5×10^{-4}	-3.8×10^{-4}
Dolomitic Principale(C2)	2.86	–	–	7.09	7.09	–	–	–	3.89	3.89	–	–	0	1.82	2.54	1.33	-3.5×10^{-4}	-3.8×10^{-4}
Werfen (2)	2.71	6.68	–	6.51	6.6	2.54	3.6	–	3.57	3.59	0.1	–	0.1	1.84	4.37	1.57	-3.5×10^{-4}	-3.8×10^{-4}
Hochwipfel (1)	2.69	6.37	–	5.77	6.07	9.89	3.54	–	3.23	3.38	0	–	0	1.79	8.75	3.12	-1.1×10^{-4}	-5.7×10^{-4}
Granodioritic orthogneiss (*)	2.71	6.04	6.35	6.20	6.19	5.0	3.37	3.51	3.55	3.48	–	–	–	1.78	4.7	2.84	-5.0×10^{-4}	-5.0×10^{-4}

Abbreviations: Vp(*x*)=Vp (km/s) measured in the *X* direction at 400 MPa. Same for Vp(*y*) and Vp(*z*); Vp(*xyz*) is the average value. Anis.(%)=seismic anisotropy in %. Vs1 is the fastest of the two perpendicularly polarized S-waves. Average pressure derivatives were calculated in the pressure range 200–450 MPa, whilst average temperature derivatives were taken from Carmichael (1989).
(*) Values taken from a sample of comparable mineralogy.

Shtrikman averaging schemes (Table 5). The results are in good agreement with the measured velocities, except for the sandstones (mainly Vs). This can be explained by a more complex mineralogical assemblage that is difficult to reproduce by the small volume of the analyzed powders.

To quantify the seismic anisotropy **A**, we used the relation proposed by Birch (1961): $\mathbf{A}\% = 100 * (Vp_{max} - Vp_{min})/Vp_{mean}$. Generally, seismic waves propagate faster along the foliation plane, except for the Fm. Calcari Grigi where the fast direction is normal to the foliation. The Paleozoic sandstone sample (1) has the strongest anisotropy (10% at 400 MPa), that can be mainly attributed to the preferred orientation of phyllosilicates (Vp anisotropy of a single crystal of mica ~60%, Alekesandrov and Ryzhova, 1961). The other lithologies have negligible anisotropy and can be considered seismically isotropic. The birefringence is relevant only in the foliation plane of the Cenozoic Flysch (Birefringence=0.2 km/s at 400 MPa).

5. Synthetic profiles

Synthetic profiles of seismic velocities and their ratio, density, elastic parameters, reflection coefficient and seismic energy (Fig. 4) were elaborated up to 22 km depth, that represents the maximum depth of the seismicity in the area (Bressan et al., 2003). The four different one-dimensional geological models S1 to S4 are located in the Prealpine belt (Fig. 1), that is the most seismic active zone of the Friuli area (Slejko et al., 1999; Bressan et al., 2003). The temperature and pressure profiles of each geological model were calculated as in Gentile et al. (2000), using the parameters listed in Table 6. Seismic velocities were then corrected for temperature and pressure according to the corresponding temperature and pressure profiles and derivatives listed in Table 3b.

We emphasize that all the velocities were measured under dry conditions, though it is well known (Nur and Simmons, 1969) that pore fluid pressure affects significantly seismic wave propagation and their ratio. The most important consequences are that in real geological settings seismic waves propagate slower due to the lower effective pressure with respect to confining pressure. In presence of pore pressure also the Vp/Vs ratio and, thus, Poisson's coefficient could be higher due to the major effect on shear waves (Nur and Simmons, 1969).

As expected from the laboratory measurements, the synthetic profiles highlight the presence of high-velocity and stiff bodies corresponding to dolomitic and Triassic calcareous rocks, lying mainly at shallow depths (0 to 2.5 km) and between 5 to 10 km depth. The Jurassic–

Table 4
Calculated elastic parameter tensors at 400 MPa for the selected lithologies' samples

Rock type	*G*				*K*				*E*				v			
	x	*y*	*z*	Mean	*x*	*y*	*z*	Mean	*x*	*y*	*z*	Mean	*x*	*y*	*z*	Mean
Cenozoic sandstone (4)	30.82	–	32.55	31.58	73.64	–	67.72	70.81	81.14	–	84.16	82.48	0.316	–	0.293	0.305
Calcari Grigi (C1)	31.38	31.76	29.71	31.01	60.56	59.06	78.86	66.74	81.10	79.09	79.18	80.55	0.280	0.277	0.333	0.299
Dolomia Principale(C2)	–	–	45.29	45.29	–	–	90.55	90.55	–	–	116.46	116.46	–	–	0.285	0.285
Werfen (2)	37.20	–	36.58	36.99	78.47	–	72.86	75.70	96.36	–	94.00	95.42	0.295	–	0.285	0.290
Hochwipfel (1)	35.72	–	29.38	32.17	67.21	–	54.58	60.86	90.10	–	74.73	82.06	0.277	–	0.272	0.275
Granodioritic orthogneiss (*)	31.70	32.33	35.88	33.30	60.86	68.15	61.70	63.57	82.40	89.82	90.16	87.46	0.274	0.280	0.256	0.270

G, *K* and *E* are the shear, bulk and elastic modulus, respectively. v is the Poisson's coefficient. Values are in MPa, except for the Poisson's coefficient that is adimensional. *see Table 3b.

Cretaceous limestone and flysch units represent minima in seismic velocities and elastic parameters and maxima for the Poisson's coefficient, because of the high Vp/Vs ratio. The Hochwipfel Fm. is characterized by low Poisson's coefficient (see Section 3). The marked differences in the elastic parameters synthetic profiles provide evidences of a high rheological contrast between stiff triassic units and Paleozoic sandstones and the Jurassic–Cretaceous limestones (Fm. Calcari Grigi) with important feedbacks in the localization of deformation.

Finally, the calculated normal incidence reflection coefficients (Fig. 5) are high at the top and the bottom of Fm. Dolomia Principale ($0.6<R<0.11$) and generally low in correspondence of the other geological contacts ($0.01<R<0.05$). According to Sheriff and Geldart (1995), the minimum reflection coefficient required by an interface to be a potential reflector in seismic profiling is 0.04; therefore, the contact between the dolomitic units and any other lithotype is probably "illuminated" by the seismic signal, while the transitions between Cenozoic sandstones and the Jurassic–Cretaceous limestone ($R=0.01$) or Paleozoic sandstones and the basement ($R<0.01$) are badly resolved. The contact between Triassic limestones and Paleozoic sandstones has an intermediate probability of being detected ($R=0.05$). We note here that the calculated reflection coefficients do not account for the considerable constructive interference due to the presence of thin layering in the proximity of a lithological discontinuity; however, we believe that these values represent a reliable characterization of the stratigraphic sequence reflectivity profile that, to a first order, depends on the bulk rock properties.

6. Discussion

A basic question debated in literature regards the discrepancies between the seismic properties measured in the laboratory and the in-situ seismic properties measured over large rock volumes. Generally, the in-situ pressure and temperature conditions, the fracturing and pore fluid pressure at scales usually not considered in the laboratory measurements can explain the differences.

The laboratory measurements are expected to provide constraints for the reconstruction of synthetic seismic models of the crust suitable also for other investigations. An important tool is the relation between the occurrence of seismicity and the crustal seismic properties. Some investigations (Zhao and Kanamori, 1993; Thurber et al., 1997; Vlahovic and Powell, 2001) have evidenced a correlation between the occurrence of seismicity and the crustal rheological boundaries marked by sharp Vp and Vs changes.

6.1. Comparison with sonic velocity data

The Vp profile calculated from values measured in the lab is compared with the Vp profile obtained in the field by means of sonic-log (Fig. 6).

The well Cargnacco 1 (Fig. 1), close to the Udine town, was drilled by the ENI-AGIP company in a relatively undeformed foreland. The Vp velocities obtained with sonic-log technique are from ENI E and P courtesy.

The stratigraphic succession (Venturini, 2002) is 7250 m thick. Mainly flysch deposits extend from surface down to 900 m depth. Below occur mainly Cretaceous–Jurassic limestones down to about 6000 m depth. A layer of upper Triassic dolomitic rocks, about 1000 m thick, is then recognized. The stratigraphic section ends with middle Triassic volcanic rocks.

In the stratigraphic synthetic profiles, we modeled the surface deposits with the sandstones of the Alpine Flysch (sample 4), the Cretaceous–Jurassic limestones with the Calcari Grigi Fm. (sample C1) and the dolomitic rocks with the Dolomia Principale Fm (sample C2).

Table 5
Calculated effective densities and velocities of the selected samples from the mineralogical composition using the Voigt, Reuss, Hill and Hashin–Shtrikman averaging schemes

Rock type	Calculated	Differences (%)	Calculated				Differences (%)				Calculated				Differences (%)			
	ρ	$\Delta\rho$	Vp(V)	Vp(R)	Vp(H)	Vp ($H-S$)	ΔV	ΔR	ΔH	$\Delta H-S$	Vs(V)	Vs(R)	Vs(H)	Vs($H-S$)	ΔV	ΔR	ΔH	$\Delta H-S$
Cenozoic sandstone (4)	2.752	−0.5	6.779	6.504	6.641	6.479	8.3	4.1	6.2	3.8	3.813	3.757	3.785	3.708	14.4	13.0	13.7	11.6
Calcari Grigi (1)	2.712	−1.6	6.539	6.539	6.539	–	5.6	5.6	5.6	–	3.435	3.435	3.435	–	3.7	3.7	3.7	–
Dolomia Principale (C2)	2.857	0.1	7.379	7.356	7.367	7.365	4.0	3.7	3.8	3.8	3.996	3.987	3.992	3.991	2.7	2.5	2.6	2.6
Werfen (2)	2.706	0.2	6.493	6.403	6.448	6.451	−1.6	−3.0	−2.3	−2.3	3.504	3.488	3.496	3.495	−2.4	−2.9	−2.7	−2.7
Hochwipfel (1)	2.722	−1.2	6.025	5.935	5.980	6.023	−0.7	−2.3	−1.5	−0.8	3.691	3.646	3.669	3.832	8.8	7.6	8.2	12.5

Differences (Δ) were calculated analoguosly to the anisotropy (see text), using velocities measured at 400 MPa. ρ is the calculate density with the Voigt averaging scheme. Vp(V), Vp(R), Vp(H) and Vp(H−S) are compressional velocities calculated using the Voigt, Reuss, Hill and Hashin–Shtrikman averaging schemes. Same for Vs. The values calculated with the Hashin–Shtrikman averaging scheme are the arithmetic average of the upper and lower bounds.

Except for the surface deposits, the velocity profiles pertaining to the limestones and dolomitic rocks match very well. This supports that our one-dimensional modelling of the calcareous–carbonatic stratigraphic sequence of the Friuli area with the calcitic veins bearing limestones and dolomitic samples analyzed in the laboratory is probably correct and that the fluids do not play an important role in this relatively undisturbed tectonic area. Furthermore, it is worth to note that calcite filled fractures are widespread in the Friuli's Cretaceous–Jurassic limestones and Triassic dolomites, a characteristic that can not be neglected when attempting to study the rock seismic properties. The observed discrepancies between laboratory and sonic-log velocities in the surface deposits are probably due to the differences in the lithological components. The deposits drilled in the well are mainly made up of clays, silstones and sandstones (Venturini, 2002) while the sample analyzed in the laboratory is a sandstone. Furthermore, the porosity of these surface deposits, measured in the well, is 35% (personal communication of ENI E and P courtesy) while the porosity of the Cenozoic sandstone sample measured in laboratory is 3.2% at ambient pressure.

6.2. Comparison with tomographic inverted velocities

The Vp and Vs data of the synthetic profiles calculated from the laboratory measurements are compared with the Vp and Vs values obtained with 3-D tomographic inversion of local earthquakes (Gentile et al., 2000), at the grid nodes close to the location of the synthetic profiles. Fig. 7 shows the location of the 3-D inversion grid, the location of the lithostratigraphic profiles and the relocated seismicity from 1984 to 2004. The 3-D Vp and Vp/Vs tomographic images of the upper Friuli crust (from surface to 12 km depth) were computed using the Thurber's method (1983) of joint inversion for hypocenters and the 3-D velocity structure from local earthquakes. The Vp tomographic images were best restored (Gentile et al., 2000) in the central part of the area, where the lithostratigraphic syntetic profiles S1, S2, S3, S4 are located (Fig. 7), at 2, 4, 6 and 8 km depth while the 3-D inverted Vp/Vs images were best restored at 4 and 6 km depth.

The geological units are characterized by the following values of tomographic P wave velocities and P- to S-velocity ratio.

Low P velocities (Vp = 5.4–5.8 km/s) and high Vp/Vs values (1.82–1.85) are related to Alpine Flysch and Quaternary deposits in the southern sector of the investigated area (Figs. 1, 7). The prevailing lithologic units, Triassic–Jurassic limestones and dolomitic rocks are characterized by P wave velocity range 5.9–6.6

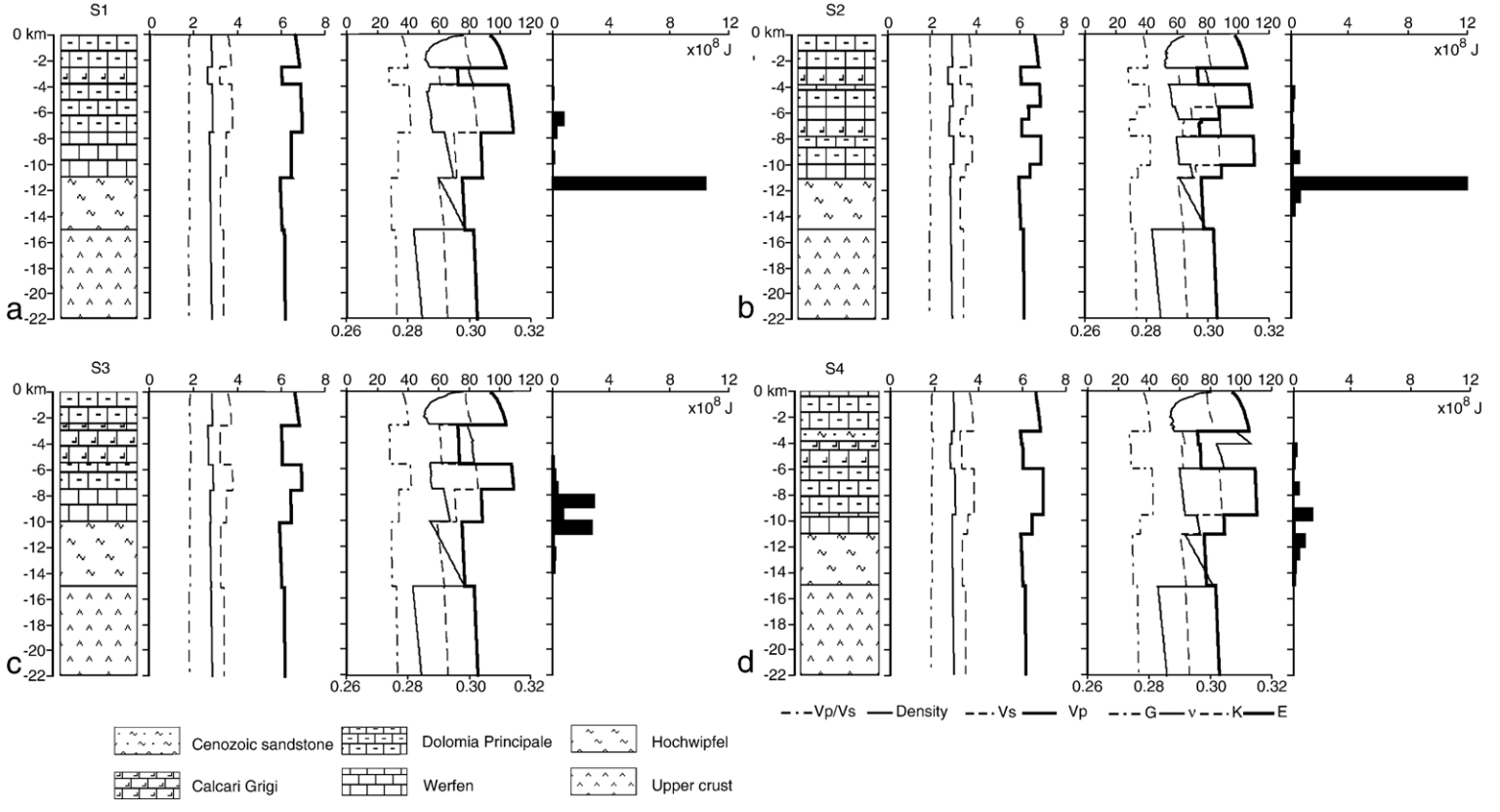

Fig. 4. Stratigraphic columns and synthetic profiles S1 (a), S2 (b), S3 (c), S4 (d) versus depth of Vp/Vs, density, Vs, Vp, elastic parameters (G, K, E, Poisson's coefficient). The histograms represent the cumulative seismic energy released by the earthquakes relocated with the 3-D tomographic model of Gentile et al. (2000). The earthquakes were selected in the range±1 km in the E–W direction and in the range±3 km in the N–S direction from the location of the lithostratigraphic synthetic profiles.

Table 6
Thermal conductivity and its pressure and temperature derivatives, heat production, pressure and temperature derivatives of density used to calculate the pressure and temperature dependence of seismic properties

Rock type	Thermal conductivity k(W m^{-1} K^{-1})	dk/dP (W m^{-1} K^{-1} Mpa^{-1})	dk/dT (W m^{-1} K^{-2})	Heat production (W m^{-3})	dDensity/dP (Mg m−3 Mpa−1)	dDensity/dT (Mg m^{-3}K^{-1})
Cenozoic sandstone (4)	2.2	4.5×10^{-4}	4.5×10^{-4}	1.2×10^{-6}	4.0×10^{-4}	5.0×10^{-5}
Calcari Grigi (C1)	6.52	4.5×10^{-4}	6.8×10^{-4}	8×10^{-7}	4.0×10^{-4}	5.0×10^{-5}
Dolomia Principale (C2)	6.52	4.5×10^{-4}	6.8×10^{-4}	8×10^{-7}	4.0×10^{-4}	5.0×10^{-5}
Werfen (2)	6.52	4.5×10^{-4}	6.8×10^{-4}	8×10^{-7}	4.0×10^{-4}	5.0×10^{-5}
Hochwipfel (1)	2.2	4.5×10^{-4}	4.5×10^{-4}	1.2×10^{-6}	4.0×10^{-4}	5.0×10^{-5}
Granodioritic orthogneiss	3.28	4.5×10^{-4}	5.0×10^{-4}	1.2×10^{-6}	4.0×10^{-5}	1.7×10^{-5}

Parameters were taken from Gentile et al. (2000) and references therein.

km/s and Vp/Vs values ranging from 1.78 to 1.88. The Vp values in the range 6.0–6.5 km/s and Vp/Vs values between 1.75 and 1.82 are related to the Paleozoic units.

The P and S wave velocities from tomographic inversion and laboratory measurements are reported in Table 7.

The laboratory velocities are generally higher than the velocities obtained with the tomographic inversion. Average differences between laboratory and tomographic Vp values are 11% (range 5.8%–14.1%) for dolomitic rocks and 3% (range 0.0%–5.5%) for Werfenian limestone, whilst are only slightly higher than tomographic Vp (1.8%) in the case of the Calcari Grigi limestones and are very similar in the case of Flysch lithology (Cenozoic sandstone).

The shear wave velocities from laboratory measurements are generally 10% higher than the tomographic Vs (range 5.0%–14.7%) for the dolomitic lithology, whilst only 1.1% (range — 3.4%–4.5%) for the Werfenian limestones. In one case (S4 profile, 10 km depth), the measured Vs of the Werfenian limestone is lower than the corresponding tomographic Vs. We point out, however, that the tomographic nodes at 10 km depth are poorly resolved. The other case of lower laboratory Vs value is that of the Flysch lithology (S4 profile), with a laboratory velocity lower of about 8.9% with respect to the tomographic velocity. The Vs values are similar for the Calcari Grigi limestones.

The observed discrepancies between the velocity profile values calculated from laboratory measurements and the ones obtained with the tomographic inversion can be attributed to many potential causes.

The different scaling aspects of the two approaches, one regarding large rock volume the other small rock samples, can contribute to the observed discrepancies. Furthermore, the small analyzed samples could be not fully representative of the in-situ whole lithological units, although, as shown in the previous section, some good constraints resulted from the direct comparison with sonic log data. The 3-D Vp and Vp/Vs tomographic images of the Friuli area are characterized by marked lateral heterogeneities, that were related to the degree of fracturing and hence to faulting geometries (Gentile et al., 2000).

Another aspect regards the uncertainties affecting the 3-D inversion for the reconstruction of the true velocity images. We recall that, on the basis of the checkerboard resolution test and restoring resolution test (Gentile et al., 2000), the Vp tomographic images were best restored for layers 2, 4, 6, and 8 km depth while the 3-D inverted Vs images were best restored in the layers 4 and 6 km depth.

6.3. Comparison with the seismicity

The velocity structure and the elastic properties of the stratigraphic synthetic profiles are compared with the depth extent of seismicity, occurred from 1984 to 2004 and located with the tomographic model of Gentile et al. (2000).

Fig. 4a–d shows the depth distribution of the cumulative seismic energy released by the earthquakes around the location of the stratigraphic synthetic profiles.

The seismic energy released E_S is estimated using the relation of Bressan et al. (2007):

$$\log_{10}E_S = 1.94M_D + 2.26$$

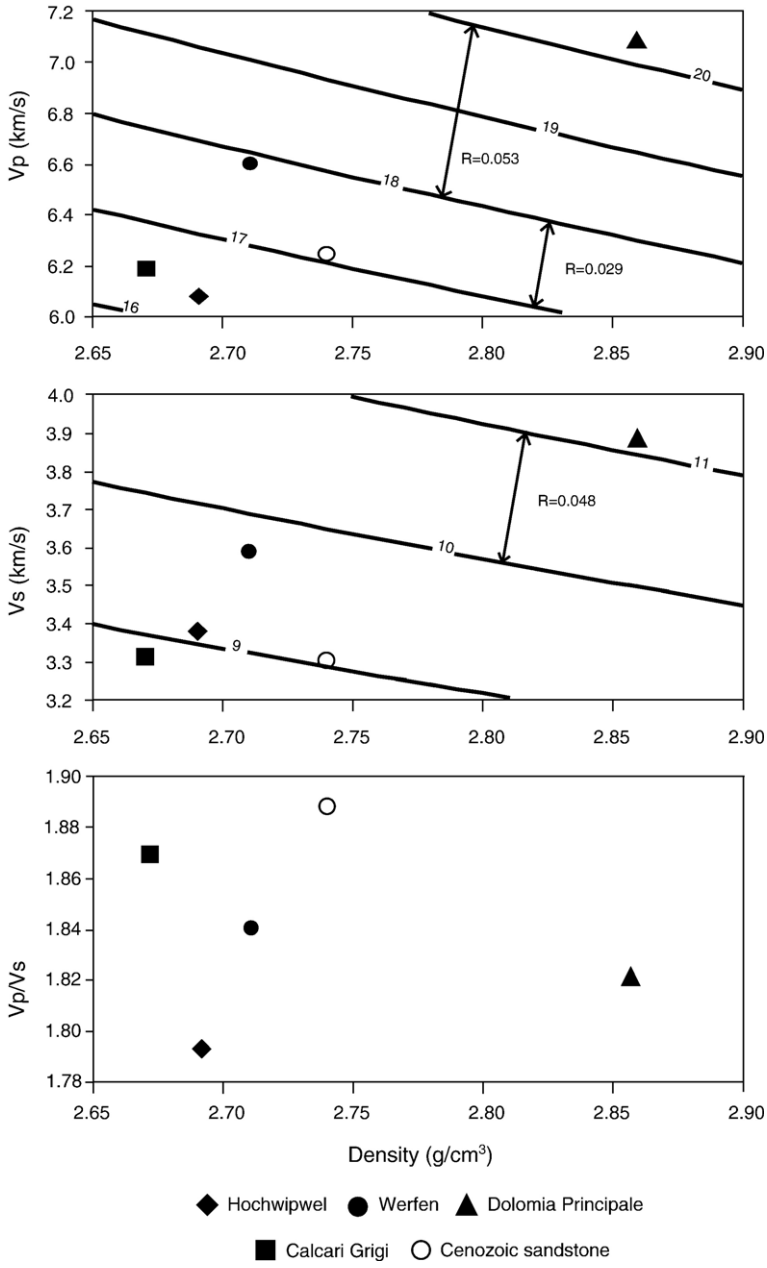

Fig. 5. Graphs showing the positive correlation between density and seismic wave velocities measured at 400 MPa. Vp/Vs ratios do not depend on density but on the mineralogy and the ages of the samples (see text). The acoustic impedance isolines are also drawn; the spacing between two or more isolines is proportional to the reflection coefficient calculated for normal incidence.

where M_D is the magnitude calculated from earthquake coda duration (Rebez and Renner, 1991).

The depth distribution of the elastic moduli (bulk, shear, Young moduli and Poisson's ratio) of the stratigraphic profiles is shown in Fig. 4. The peaks of the released seismic energy are related to the boundaries between layers of different lithology, marked by sharp variations of the elastic moduli. In particular, the maximum peaks are located between 10 and 12 km depth, corresponding to the lithological constrast between Paleozoic units and Werfenian limestones (S1, S2, S3, and S4 profiles) and between 8 and 10 km depth (S3, S4 profiles) where the lithology changes from dolomitic rocks to Werfenian limestones. Minor seismicity appears to be connected, at least partly, to the lithological changes. In synthesis, the deformation

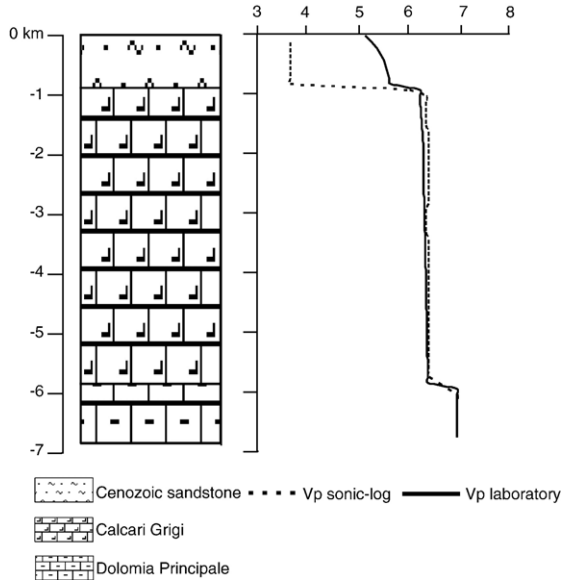

Fig. 6. Well Cargnacco 1. Modeled stratigraphic column and synthetic Vp profile (bold line) calculated from lab measurements. The Vp velocities (dotted) measured with sonic-log technique (ENI E and P courtesy) are also shown.

appears to localize at rheological boundaries rather than in weak material units as results also at small scale investigations (Mancktelow and Pennacchioni, 2005).

7. Conclusions

We investigated the seismic properties of the upper crust of the central Friuli area (northeastern Italy) with laboratory measurements. The experimental data provided significant constraints for the elaboration of the synthetic geophysical–stratigraphic profiles. The conclusions can be summarized as follows.

At 400 MPa confining pressure the dolomitic rock shows the highest velocities: Vp ~7 km/s, Vs ~3.6 km/s. The limestones are characterized by intermediate velocities (Vp ~6.3 km/s, Vs ~3.5 km/s) and the Paleozoic and Cenozoic sandstones have the lowest velocities (Vp ~6.15 km/s, Vs ~3.35 km/s).

The anisotropy is negligible for all the samples, except the Paleozoic sandstones that are characterized by 10% anisotropy at 400 MPa. The birefringence is relevant only in the foliation plane of the Cenozoic Flysch.

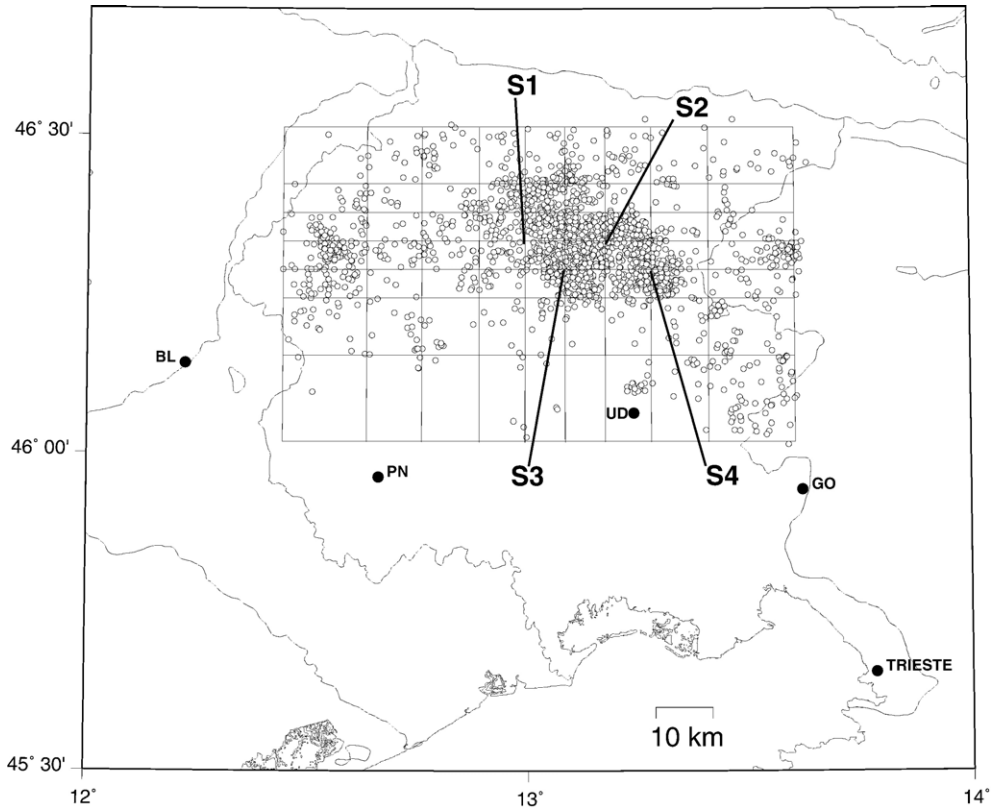

Fig. 7. Location of the 3-D Vp and Vp/Vs inversion grid of Gentile et al. (2000) with the relocated seismicity (circles), recorded from 1984 to 2004 by the INOGS local seismic array. The location of the stratigraphic synthetic profiles S1, S2, S3 and S4 is shown. BL: Belluno; PN: Pordenone; UD: Udine; GO: Gorizia.

Table 7
Comparison between Vp and Vs velocities obtained from 3-D tomografic inversion (tom) and calculated from lab measurements (lab)

Profile	Depth	Vp tom	Vp lab	Vs tom	Vs lab	Lithology (Fm)
S1	0	5.88	6.67	3.17	3.57	Dolomia P.
S1	2	5.89	6.82	3.18	3.73	Dolomia P.
S1	4	6.25	6.92	3.52	3.78	Dolomia P.
S1	6	6.50	6.96	3.57	3.80	Dolomia P.
S1	8	6.19	6.48	3.35	3.51	Werfenian
S1	10	6.29	6.49	3.46	3.50	Werfenian
S2	0	6.02	6.71	3.26	3.64	Dolomia P.
S2	2	6.14	6.85	3.34	3.75	Dolomia P.
S2	4	6.14	6.94	3.36	3.79	Dolomia P.
S2	6	6.28	6.43	3.38	3.50	Werfenian
S2	8	6.29	7.00	3.46	3.80	Dolomia P.
S2	10	6.59	7.00	3.61	3.80	Dolomia P.
S3	0	6.09	6.67	3.27	3.57	Dolomia P.
S3	2	5.91	6.82	3.19	3.73	Dolomia P.
S3	4	5.97	6.08	3.23	3.24	Calcari Grigi
S3	6	6.08	6.96	3.42	3.80	Dolomia P.
S3	8	6.12	6.48	3.49	3.51	Werfenian
S3	10	6.31	6.49	3.48	3.50	Werfenian
S4	0	5.78	6.67	3.16	3.57	Dolomia P.
S4	2	5.89	6.82	3.29	3.73	Dolomia P.
S4	4	6.07	6.01	3.43	3.15	Flysch
S4	6	6.22	7.00	3.41	3.81	Dolomia P.
S4	8	6.01	7.00	3.30	3.81	Dolomia P.
S4	10	6.49	6.49	3.63	3.51	Werfenian

The corresponding geological formations (Fm) are reported in the column Lithology. Dolomia Principale Fm: upper Triassic dolomitic rocks; Werfen Fm: Lower Triassic limestones; Calcari Grigi Fm.: Jurassic limestones; Flysch: Cenozoic sandstones.

The elaborated synthetic profiles of seismic velocities, their ratio, the density and the elastic parameters highlight the presence of stiff bodies corresponding to Triassic dolomitic and calcareous rocks. High rheological contrasts are observed between stiff Triassic units and soft sandstones and the Jurassic limestones. The reflection coefficients are high at top and the bottom of Fm. Dolomia Principale ($0.6<R<0.11$) and generally low in correspondence of the other geological contacts ($0.01<R<0.05$).

The Vp profile elaborated from laboratory measurements and the Vp in-situ profile obtained by sonic log match very well for limestones and dolomitic lithology. This comparison supports the validity of our one-dimensional modelling of the calcareous-carbonatic stratigraphic sections that are the dominant lithologies in the upper crust of the central Friuli area. It suggests also that the influence of fluids seems not dominant.

The comparison of the Vp and Vs values of the synthetic profiles with the Vp and Vs values obtained from the 3-D tomographic inversion of local earthquakes evidences that the laboratory Vp are generally higher than the tomographic ones. Major discrepancies are observed for the dolomitic lithology, also for shear wave velocities. In the other cases, the laboratory shear wave velocities and the corresponding tomographic ones are nearly similar. The laboratory Vs is considerably lower only for Flysch lithology.

The comparison between the velocity structure and the elastic properties of the synthetic profile with the depth location of the seismicity shows that the released seismic energy is mainly located at rheological boundaries, in correspondence of layer boundaries, marked by sharp variations of velocities and elastic moduli.

Acknowledgements

The Vp velocities of the well Cargnacco are furnished for ENI E and P courtesy. We are indebted with C. Venturini for his precious information about the stratigraphy of the Friuli area and the provision of the rock samples. G.F. Gentile relocated the earthquakes and thanks are due also to S. Urban for help in graphics. We thank C. Barnaba for the useful discussion about the one-dimensional geological. Constructive reviews by two anonymous reviewers is greatla appreciated. This work benefits of the stimulating discussions with R. De Franco. Dr. V. Barberini is thanked for the XRD analysis. The experiments were conducted thanks to the R'equip NF funds n. #2160-053289.98. M. Faccenda was supported at ETH Zurich by the ERASMUS program.

References

Alekesandrov, K.S., Ryzhova, T.V., 1961. The elastic properties of rock-forming minerals, II: layered silicates, Izv. Acad. Sci. USSR, Geophys. Ser. 2, 186–189.

Bass, J.D., 1995. Elasticity of minerals, glasses and melts. In: Ahrens, T.J. (Ed.), Mineral Physics and crystallography. A handbook of physical constants. AGU reference shelf, vol. 2, pp. 45–63.

Birch, F., 1960. The velocity of compressional waves in rocks to 10 kilobars (Part 1). J. Geophys. Res. 65, 1083–1102.

Birch, F., 1961. The velocity of compressional waves in rocks to 10 kilobars (Part 2). J. Geophys. Res. 66, 2199–2224.

Bosellini, A., 2004. The western passive margin of Adria and its carbonate platforms. In: Crescenti, V., D'Offizi, S., Merlino, S., Sacchi, L. (Eds.), Geology of Italy, special volume of the Italian Geological Society for the IGC 32 Florence-2004, pp. 79–92.

Bressan, G., Bragato, P.L., Venturini, C., 2003. Stress and strain tensors based on focal mechanisms in the seismotectonic framework of the Friuli–Venezia Giulia region (Northeastern Italy). Bull. Seismol. Soc. Am. 93, 1280–1297.

Bressan, G., Kravanja, S., Franceschina, G., 2007. Source parameters and stress release of seismic sequences occurred in the Friuli–Venezia Giulia region (Northeastern Italy) and in Western Slovenia. Phys. Earth Planet. Inter. 160, 192–214.

Burke, M.M., 1987. Compressional wave velocities in rocks from the Ivrea–Verbano and Strona–Ceneri zones, Southern Alps, Northern

Italy: implications for models of crustal structure, M.S. thesis, p. 78, Univ. of Wyoming, Laramie.
Burlini, L., Kunze, K., 2000. Fabric and Seismic Properties of Carrara Marble Mylonite. Phys. Chem. Earth, Part A Solid Earth Geod. 25 (2), 133–139.
Carmichael, R.S., 1989. Practical Hanbook of physical properties of rocks and minerals. CRC Press, Inc., Boca Raton, U.S.A. 741 pp.
Carulli, G.B., Ponton, M., 1992. Interpretazione strutturale profonda del settore centrale carnico-friulano. Studi Geol. Camerti 2, 275–284 CROP1-1A.
Castellarin, A., 1979. Il problema dei raccorciamenti crostali nel Sudalpino. Rend. Soc. Geol. Ital. 1, 21–23.
Cati, A., Sartorio, D., Venturini, S., 1987. Carbonate platforms in the subsurface of the northern Adriatic area. Mem. Soc. Geol. Ital. 40, 295–308.
Dey-Barsukov, S., Dürrast, S., Rabbel, H., Siegesmund, W., Wende, S., 2000. Aligned fractures in carbonate rocks: laboratory and in situ measurements of seismic anisotropy. Int. J. Earth Sci. 88, 829–839.
Ferrill, D.A., Morris, A.P., Evans, M.A., Burkhard, M., Groshong Jr., R.H., Onasch, C.M., 2004. Calcite twin morphology: A low-temperature deformation geothermometer. J. Struct. Geol. 26, 1521–1529.
Fountain, D.M., 1976. The Ivrea–Verbano and Strona–Ceneri zones, northern Italy: a cross section of the continental crust — new evidence from seismic velocities. Tectonophysics 33, 145–166.
Gentile, G.F., Bressan, G., Burlini, L., De Franco, R., 2000. Three — dimensional Vp and Vp/Vs models of the upper crust in the Friuli area (Northeastern Italy). Geophys. J. Int. 141, 457–478.
Kern, H., Burlini, L., Ashchepkov, I.V., 1996. Fabric-related seismic anisotropy in upper mantle xenoliths: evidence from measurements and calculations. In: Mainprice, D.M., Voucher, A., Vinnik, L. (Eds.), Dynamic of Subcontinental Mantle: from Seismic Anisotropy to Mountain Building. Phys. Earth Planet. Interiors, vol. 95, pp. 195–209.
Larson, A.C., Von Dreele, R.B., 2004. General Structure Analysis System (GSAS). Los Alamos National Laboratory Report LAUR, pp. 86–748.
Mancktelow, N., Pennacchioni, G., 2005. The control of precursor brittle fracture and fluid–rock interaction on the development of single and paired ductile shear zones. J. Struct. Geol. 27, 645–661.
Martinis, B.,1993. Storia geologica del Friuli. Ed. La Nuova Base-Udine, pp 268.
Mavko, G., Mukerji, T., Dvorkin, J., 1998. Rock Physics Handbook. University Press, Cambridge, p. 339.
Mazzoli, C., Sassi, R., Burlini, L., 2002. Experimental study of the seismic properties of the Eastern Alps (Italy) along the Aurina–Tures–Badia valleys transect. Tectonophysics 354, 179–194.
Merlini, S., Doglioni, C., Fantoni, R., Ponton, M., 2002. Analisi strutturale lungo un profilo geologico tra la linea Fella-Sava e l'avampaese adriatico (Friuli Venezia Giulia — Italia). Mem. Soc. Geol. Ital. 57, 293–300.
Nur, A., Simmons, G., 1969. The effect of saturation on velocity in low porosity rocks. Earth Planet. Sci. Lett. 7, 183–193.
Pickett, G.R., 1963. Acoustic character logs and their applications in formation evaluation. J. Pet. Technol. 659–667 (June).
Poli, M.E., Peruzza, L., Rebez, A., Renner, G., Slejko, D., Zanferrari, A., 2002. New seismotectonic evidence from the analysis of the 1976–1977 and 1977–1999 seismicity in Friuli (NE Italy). Boll. Geofis. Teor. Appl. 43 (1-2), 53–78.
Rasolofosaon, P.N.J., Rabbel, W., Siegesmund, S., Vollbrecht, A., 2000. Characterization of crack distribution: fabric analysis versus ultrasonic inversion. Geophys. J. Int. 141, 413–424.
Rebez, A., Renner, G., 1991. Duration magnitude for the northeastern Italy seismometric network. Boll. Geofis. Teor. Appl. 33, 177–186.
Rudnick, R.L., Fountain, D.M., 1995. Nature and composition of the continental Crust: A lower crustal perspective. Rev. Geophys. 33, 267–309.
Scarascia, S., Cassinis, R., 1997. Crustal structures in the central-eastern Alpine sector: a revision of the available DSS data. Tectonophysics 271, 157–188.
Sheriff, E.R., Geldart, P.L., 1995. Exploration Seismology, 2nd ed. Univ. Press, Cambridge. 592 pp.
Siegesmund, S., 1996. The significance of rock fabrics from the geological interpretation of geophysical anisotropies. Geotekton. Forsch. 85, 1–123.
Slejko, D., Carulli, G.B., Nicolich, R., Rebez, A., Zanferrari, A., Cavallin, A., Doglioni, C., Carraro, F., Castaldini, D., Iliceto, V., Semenza, E., Zanolla, C., 1989. Seismotectonics of the Eastern Southern-Alps: a review. Boll. Geofis. Teor. Appl. 31 (122), 109–136.
Slejko, D., Neri, G., Orozova, I., Renner, G., Wyss, M., 1999. Stress field in Friuli (NE Italy) from fault plane solutions of activity following the 1976 main shock. Bull. Seismol. Soc. Am. 89 (4), 1037–1052.
Tatham, R.H., McCormack, M.D., 1991. Multicomponent seismology in petroleum exploration. Society of Exploration Geophysicists, Tulsa.
Thurber, C.H., 1983. Earthquake locations and three-dimensionale crustal structure in the Coyote lake area, Central California. J. Geophys. Res. 88, 8226–8236.
Thurber, C., Roecker, S., Ellsworth, W., Chen, Y., Lutter, W., Sessions, R., 1997. Two dimensional seismic image of the San Andreas fault in the Northern Gablilan range, central California: evidence for fluids in the fault zone. Geophys. Res. Lett. 24 (13), 1591–1594.
Toby, B.H., 2001. EXPGUI, a graphical user interface for GSAS. J. Appl. Crystallogr. 34, 210–213.
Vai, G.B., Venturini, C., Carulli, G.B., Zanferrari, A., 2002. Alpi e Prealpi Carniche e Giulie. Friuli Venezia Giulia. Guide Geologiche Regionali. Soc. Geol. Ital. 390.
Venturini, C., 1991. Cinematica neogenico-quaternaria del Sudalpino orientale (settore friulano). Studi Geol. Camerti, Vol. Spec. Camerino (MC), pp. 109–116.
Venturini, S., 2002. Il pozzo Cargnacco 1: un punto di taratura stratigrafica nella pianura friulana. Mem. Soc. Geol. Ital. 57, 11–18.
Vlahovic, G., Powell, C.A., 2001. Three-dimensional S wave velocity structure and Vp/Vs ratios in the New Madrid Seismic zone. J. Geophys. Res. 106 (B7), 13,501–13,513.
Wepfer, W.W., Christensen, N.I., 1991. A seismic velocity confining pressure relation, with application. Int. J. Rock Mech. Min. Sci. Geomech. Abstr. 28 (5), 451–456.
Zhao, D., Kanamori, H., 1993. The 1992 Landers earthquake sequence: earthquake occurrence and structural heterogeneities. Geophys. Res. Lett. 20 (11), 1,083–1,086.